

in complete disagreement with experimental results. Conversely, a difference $\delta r = 0.5$ fm would give a negligible splitting. So the compatibility of $\delta r \approx 0.1 - 0.2$ fm with the results on ΔE is very satisfactory and may be considered as further evidence of the existence of the "halo" of the neutrons in the heavy region.

In this respect it would be very interesting to measure the isospin splitting in Ca isotopes in order to analyze the effect on ΔE of the anomalous behavior of δr in this region.¹⁹

Finally we remember that ΔE also depends on β . Our assumption on β is firmly justified,^{7,9} since on very general grounds we have⁹ $1.2 \leq \beta \leq 1.6$. Any value smaller than the one we assume would increase ΔE and would suggest an even more pronounced neutron "halo." Conversely, even the extreme value $\beta = 1.9$ is not sufficient to explain the experimental data on ΔE for heavy nuclei without the introduction of $\delta r > 0$. (We have for ^{208}Pb , $U = 150$ with $\delta r = 0$ and $\beta = 1.9$.)

¹R. Leonardi and M. Rosa-Clot, Phys. Rev. Lett. **23**, 874 (1969).

²K. Shoda and collaborators (Tohoku), private communication.

³R. Bergère and collaborators (Saclay), private communication.

⁴G. W. Greenlees, W. Mokofske, and G. J. Pyle, Phys. Rev. C **1**, 1145 (1970).

⁵E. H. Auerbach, H. M. Qureshi, and M. M. Stern-

heim, Phys. Rev. Lett. **21**, 162 (1968).

⁶However, in Ref. 1 a factor $\frac{1}{3}$ has been forgotten in the definition of r_s^2 and A_s . Further, in the definition of A_t , $3A_s$ must be replaced with $2A_s$.

⁷J. S. Levinger and H. A. Bethe, Phys. Rev. **78**, 115 (1950).

⁸M. Danos and E. G. Fuller, Annu. Rev. Nucl. Sci. **15**, 29 (1965).

⁹M. Gell-Mann, M. L. Goldberger, and W. E. Thirring, Phys. Rev. **95**, 1612 (1959).

¹⁰A. Bohr and B. R. Mottelson, *Nuclear Structure* (Benjamin, New York, 1969), Vol. I.

¹¹J. S. O'Connell, B. F. Gibson, and E. Hayward, private communication.

¹²R. Leonardi and M. Rosa-Clot, Riv. Nuovo Cimento **1**, 1 (1971).

¹³B. C. Cook, R. C. Morrison, and F. H. Chamber, Phys. Rev. Lett. **25**, 685 (1970).

¹⁴E. M. Diener, J. F. Amann, and R. Paul, Phys. Rev. C **3**, 2303 (1971); P. Paul, J. F. Amann, and K. A. Snover, Phys. Rev. Lett. **27**, 1013 (1971).

¹⁵S. C. Fultz *et al.*, Phys. Rev. C **4**, 149 (1971).

¹⁶M. Hasinoff *et al.*, Phys. Lett. **30B**, 337 (1969).

¹⁷Recently R. Ö. Akyüz and S. Fallieros, Phys. Rev. Lett. **27**, 1016 (1971), performed a calculation in the framework of the particle-hole model. They estimate $U \approx 60$ MeV. See this paper for references and a discussion of the shell-model approach to this problem.

¹⁸A special discussion is necessary for Mg^{26} and probably for Zn^{64} (Refs. 13 and 15). The spectacular splitting found in these nuclei is probably a deformation effect also. Formally a much greater value of U is obtained if one assumes $\langle r_p^2 \rangle > \langle r_n^2 \rangle$ for these nuclei.

¹⁹J. P. Schiffer, J. A. Nolen, and N. Williams, Phys. Lett. **29B**, 399 (1969).

Ratio of the $^4\text{He}(\gamma, p)$ and $^4\text{He}(\gamma, n)$ Cross Sections

W. R. Dodge and J. J. Murphy, II*

National Bureau of Standards, Washington, D. C. 20234

(Received 24 January 1972)

The $^4\text{He}(\gamma, p)^3\text{H}$ and $^4\text{He}(\gamma, n)^3\text{He}$ cross sections have been determined with a magnetic spectrometer in the energy interval of 30.0 to 51.8 MeV. We find that the average value of $\sigma(\gamma, p)/\sigma(\gamma, n)$ is 1.03 ± 0.04 in the above energy interval. The $^4\text{He}(\gamma, p)$ cross section decreases from 1.52 ± 0.13 mb at 31.7 MeV to 0.36 ± 0.03 mb at 51.8 MeV.

The equality of the $^4\text{He}(\gamma, p)$ and $^4\text{He}(\gamma, n)$ total cross sections was first established by Gorbunov and Spiridonov¹ using a cloud chamber and synchrotron bremsstrahlung radiation. Fuller's² $^4\text{He}(\gamma, p)^3\text{He}$ data and Livesey and Main's³ $^4\text{He}(\gamma, n)^3\text{He}$ data, and later measurements of Gorbunov⁴ and Main,⁵ corroborated Gorbunov's¹ original measurements. However, two recent measurements of the $^4\text{He}(\gamma, n)$ cross section have raised

serious doubts about the equality of the $^4\text{He}(\gamma, p)$ and $^4\text{He}(\gamma, n)$ cross sections. A measurement of the $^4\text{He}(\gamma, n)$ cross section by Berman, Fultz, and Kelly⁶ (BFK), when compared with the $^4\text{He}(\gamma, p)$ cross section measured by Meyerhof, Suffert, and Feldman,⁷ indicates that the average $^4\text{He}(\gamma, p)$ cross section is 1.806 ± 0.025 times as large as the average $^4\text{He}(\gamma, n)$ cross section in the energy interval between threshold and 31 MeV. Busso

*et al.*⁸ obtained results similar to those of BFK.

Few, if any, theoretical treatments of the ⁴He photodisintegration anticipated an inequality of the (γ, p) and (γ, n) cross sections of the magnitude indicated by BFK. They conjectured that either there was considerable isospin mixing of the giant dipole states in ⁴He or that charge symmetry was broken in ⁴He. Gibson,⁹ *a posteriori*, has been able to reproduce both the behavior of the (γ, n) angular distribution asymmetry term and the BFK ratio of (γ, p) to (γ, n) cross sections by judiciously mixing the continuum $J^\pi = 1^-, T = 0, T = 1$ states. As BFK pointed out, the conjecture of breaking of charge symmetry to the extent necessary to explain their results (ratio of intensities of charge-symmetry-breaking force to charge-symmetry-nonbreaking force of 2.3%) contradicts Henley's¹⁰ value of $(0.25 \pm 0.8)\%$ in ⁴He deduced from an analysis of low-energy scattering data.

Reported here is an experiment in which the

(γ, p) and (γ, n) cross sections were determined nearly simultaneously with the same apparatus.¹¹ The use of the same apparatus to measure both the (γ, p) and (γ, n) cross sections avoided the errors inherent in the comparison of two independently determined absolute cross sections. We used a magnetic spectrometer to determine the ³H and ³He yields at 90° in the laboratory system produced by electrons incident on a gaseous ⁴He target. These electrodisintegration yields were converted into ⁴He(γ, p) and ⁴He(γ, n) cross sections.¹² We find that $\sigma(\gamma, p)/\sigma(\gamma, n)$ is 1.08 ± 0.09 at 31.7 MeV and that the average value of this ratio is 1.03 ± 0.04 in the energy interval of 30.0 to 51.8 MeV.

A gaseous ⁴He target with 0.005-g/cm² stainless-steel electron beam entrance and exit windows and either a 0.00036- or 0.0006-g/cm² polyethylene terephthalate (C₁₀H₈O₄-Mylar) particle exit window was bombarded with 90-MeV electrons. The spectrometer magnet was a $2\pi/3$,

TABLE I. Summary of the results of this experiment and the data for calculating $\sigma(\gamma, p)/\sigma(\gamma, n)$. The angular-distribution coefficients $A(k_\gamma)$, $B(k_\gamma)$, and $C(k_\gamma)$ are from Meyerhof, Suffert, and Feldman,^a Perry and Bame,^b Berman, Fultz, and Kelly,^c and Gorbunov.^d In those columns in which there are two entries, the upper entry refers to the ⁴He(γ, p) reaction and the lower to the ⁴He(γ, n) reaction. The uncertainties of σ include only the errors in the angular-distribution coefficients and uncertainties due to counting statistics. T' and T are the particle kinetic energies before and after correction for energy loss in the ⁴He gas and the target cell wall.

k (MeV)	$A(k_\gamma)/B(k_\gamma)^e$	$C(k_\gamma)/B(k_\gamma)^e$	R_e/R_γ	T (MeV)	T' (MeV)	Relative Counting Efficiency	θ Degrees	$d\sigma_\gamma/d\Omega)^{c, m}$ $\mu\text{b}/\text{sr}$	σ_γ mb	$\frac{\sigma(\gamma, p)}{\sigma(\gamma, n)}$
29.8 ^f	.016 \pm .005 .12 \pm .08	-.53 \pm .11 .22 \pm .15	1.017	2.392 2.202	2.213 1.355	1.00 .83	100.1 101.6	202 \pm 4. 159 \pm 25.	1.61 \pm .06 1.54 \pm .34	1.07 \pm .24
31.7 ^f	.016 \pm .005 .038 \pm .028	-.60 \pm .05 .30 \pm .13	1.005	2.856 2.665	2.631 1.594	1.00 .90	100.6 101.0	173 \pm 4. 127 \pm 17.	1.40 \pm .04 1.19 \pm .17	1.18 \pm .16
31.7 ^g	.016 \pm .005 .038 \pm .028	-.60 \pm .05 .30 \pm .13	1.005	2.856 2.665	2.631 1.594	1.00 .90	100.6 101.0	192 \pm 9. 159 \pm 16.	1.54 \pm .14 1.48 \pm .15	1.04 \pm .12
33.9 ^g	.0 .04 \pm .03	-.66 \pm .07 .34 \pm .10	1.020	3.294 3.104	3.092 2.181	1.00 .98	100.4 100.7	168 \pm 8. 131 \pm 13.	1.30 \pm .10 1.24 \pm .17	1.05 \pm .17
31.7 ^h	.016 \pm .005 .038 \pm .028	-.60 \pm .05 .30 \pm .13	1.005	2.856 2.665	2.558 1.165	1.00 .80	100.6 101.0	192 \pm 11. 164 \pm 45.	1.51 \pm .12 1.53 \pm .51	.98 \pm .33
33.5 ^h	.0 .04 \pm .03	-.67 \pm .07 .35 \pm .10	1.037	3.392 3.201	3.131 1.975	1.00 .93	100.4 100.7	150 \pm 6. 117 \pm 6.	1.16 \pm .10 1.10 \pm .14	1.05 \pm .16
35.2 ^h	.0 .04 \pm .03	-.70 \pm .07 .46 \pm .13	1.039	3.708 3.517	3.464 2.400	1.00 1.00	100.3 100.6	137 \pm 5. 104 \pm 5.	1.05 \pm .04 1.00 \pm .08	1.05 \pm .09
37.1 ^h	.0 .04 \pm .03	-.75 \pm .09 .47 \pm .07	1.022	4.170 3.980	3.947 2.985	1.00 1.00	100.3 100.5	105 \pm 3. 81 \pm 3.	.80 \pm .03 .78 \pm .05	1.03 \pm .08
44.3 ^h	.0 .04 \pm .03	-.84 \pm .07 .34 \pm .04	1.020	5.916 5.726	5.746 5.000	1.00 1.00	100.3 100.4	74 \pm 3. 61 \pm 3.	.56 \pm .02 .55 \pm .03	1.01 \pm .07
51.8 ^h	.0 .0	-.96 \pm .10 .06 \pm .03	1.022	7.680 7.539	7.541 6.961	1.00 1.00	100.5 100.6	51 \pm 3. 43 \pm 1.3	.36 \pm .02 .36 \pm .01	1.00 \pm .08

^aSee Ref. 7.

^bSee Ref. 14.

^cSee Ref. 6.

^dSee Ref. 4.

^eAngular-distribution coefficients for the ⁴He($\gamma, ^3\text{H}$) and ⁴He($\gamma, ^3\text{He}$) reactions.

^f0.00036-g/cm² Mylar window 3.81 cm long and 1.27 cm wide.

^g0.00036-g/cm² Mylar window 1.587 cm in diameter with a 0.953-cm collimator.

^h0.0006-g/cm² Mylar window 1.587 cm in diameter with a 0.953-cm collimator.

double-focusing magnetic wedge. Ten $0.1 \times 1.0 \times 6.0\text{-cm}^3$ lithium-drifted silicon p-i-n semiconductor detectors were mounted in the focal plane of the magnet and were cooled to 77°K to insure an optimum detection efficiency. The relative detection efficiency of our detector system for α particles was measured with a ^{210}Po α -particle source and energy degrading absorbers. We assumed that the relative area of the counts/unit magnetic field as a function of the magnetic field was equal to the counting efficiency at the mean α -particle energy. The average of the relative detection efficiencies of all detectors at mean α -particle energies of 0.53, 1.50, 2.10, 2.93, and 5.303 MeV were $0.62^{+0.13}_{-0.03}$, 0.76 ± 0.02 , 0.93 ± 0.01 , 98 ± 0.01 , and 1.00, respectively. The detection efficiencies listed in Table I were obtained from the α -particle values $\mathcal{E}_\alpha(T_\alpha)$ by assuming that, for a particle of mass A , charge Z , and kinetic energy T , the efficiency is given by $\mathcal{E}(T) = \mathcal{E}_\alpha(T_\alpha = \eta T)$, where $\eta = (Z_\alpha/Z)^2 A_\alpha/A$. It was also assumed that the absolute efficiency for 5.303-MeV α particles was 100%. These assumptions give what are believed to be upper limits to the efficiencies. Taking $\eta = 1$ as a lower limit reduces the cross-section ratio at the most sensitive energy (29.8 MeV) by 8%. The (γ, n) cross section is increased by 10%.

Figures 1(a) and 1(b) show pulse-height spectra used to determine the $^4\text{He}(e, ^3\text{H})e'p$ and $^4\text{He}(e, ^3\text{He})e'n$ yields, respectively, at $k_\gamma = 31.7$ MeV. The spectrometer magnetic field was programmed so that (γ, p) and (γ, n) cross sections at a given photon energy were always measured within a time interval of approximately 2 h.

The similarities between electrodisintegration and photodisintegration cross sections and their differences have been discussed extensively in the literature.^{12,13} Briefly, if a photodisintegration cross section is given by

$$d\sigma_\gamma/d\Omega = A(k_\gamma) + B(k_\gamma) \sin^2\theta + C(k_\gamma) \sin^2\theta \cos\theta, \quad (1)$$

then the electrodisintegration cross section is given by

$$d\sigma_e/d\Omega = (\alpha/\pi) \left\{ [(1+R^2) \ln\lambda - 2R] A(k_0) + R^2 B(k_0) - \frac{1}{3} R_k R (1+R) C(k_0) \cos\theta [(1+R^2) \ln\lambda - 2R - \frac{3}{2} R^2] \right. \\ \left. \times B(k_0) \sin^2\theta + [(1+R^2) \ln\lambda + R_k (-1 + \frac{1}{2}R + \frac{11}{8}R^2)] C(k_0) \sin^2\theta \cos\theta \right\}. \quad (2)$$

Here θ is the angle between the detected particle and the incident electron in the center-of-mass system; E_i and E_f are the total energies of the incident and scattered electrons, respectively; $R = E_f/E_i$, $R_k = E_f/(E_i - E_f) = E_f/k_0$; and $\lambda = 2E_0 R_k/m_e$. The real and virtual photon energies are k_γ and k_0 . Column 4 (R_e/R_γ), Table I, shows the extent to which the ratio of ^3H and ^3He electrodisintegration yields differs from the ratio of ^3H and ^3He photodisintegration yields.

The results of our experiment are summarized in Table I. The total cross section σ was derived

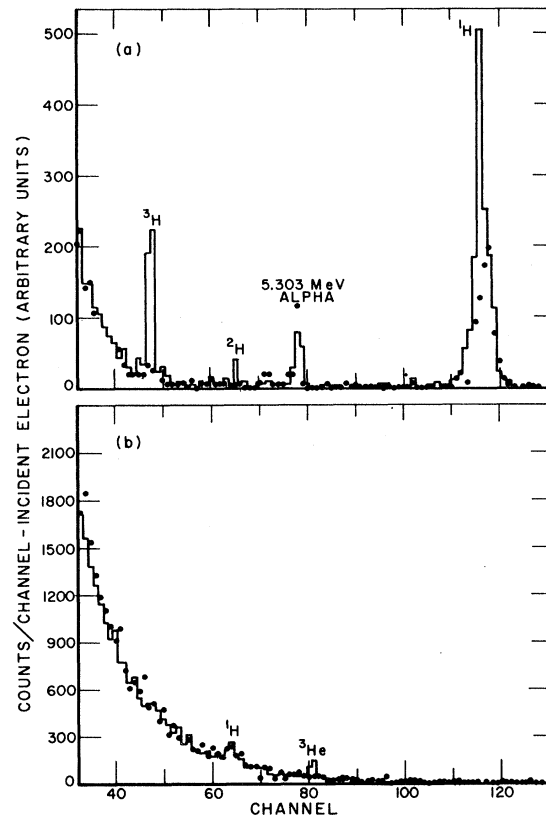


FIG. 1. (a) A focal-plane-detector pulse-height spectrum from which the $^4\text{He}(e, ^3\text{H})e'p$ yield was determined at $k_\gamma = 31.7$ MeV. The α particles are from ^{210}Po deposited on the detector. (b) A focal-plane-detector pulse-height spectrum from which the $^4\text{He}(e, ^3\text{He})e'n$ yield was determined at $k_\gamma = 31.7$ MeV. Both spectra were obtained using a ^4He gas cell with a 0.00036-g/cm^2 Mylar window and are from the same detector but with different amplifier gains. Histograms, taken with a cell filled with ^4He ; circles, taken with an identical empty cell.

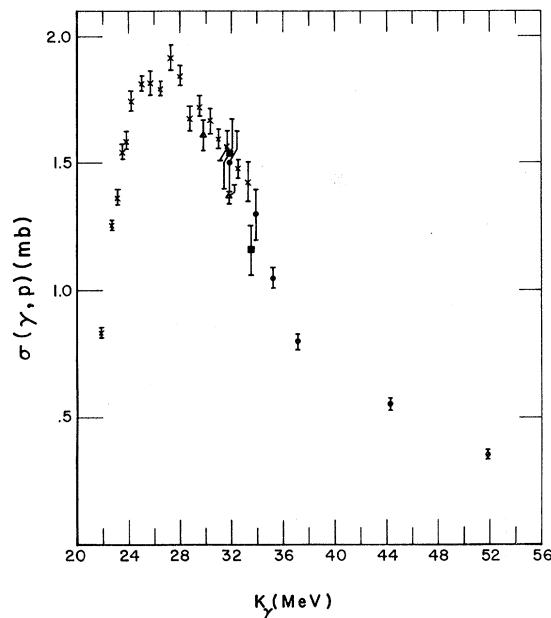


FIG. 2. The ${}^4\text{He}(\gamma, p){}^3\text{H}$ total cross section as a function of k . Crosses, results of Meyerhof, Suffert, and Feldman (Ref. 7); circles, our results using a 0.0006-g/cm² Mylar window 1.587 cm in diameter; squares, our results using a 0.00036-g/cm² Mylar window 1.587 cm in diameter; triangles, our results using a 0.00036-g/cm² Mylar window 3.81 cm long and 1.27 cm wide.

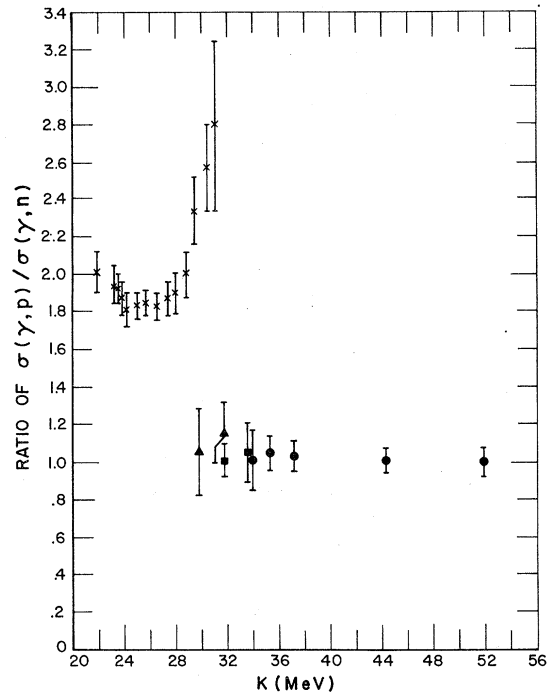


FIG. 3. The ratio $\sigma(\gamma, p)/\sigma(\gamma, n)$. The crosses are the results calculated by Berman, Fultz, and Kelly (Ref. 6) using the $\sigma(\gamma, p)$ values of Meyerhof, Suffert, and Feldman (Ref. 7). The other symbols are defined in Fig. 2.

from $[d\sigma/d\Omega]_{c.m.}$ by assuming that

$$\sigma = \frac{8\pi}{3} \frac{\frac{3}{2}A(k_\gamma) + B(k_\gamma)}{A(k_\gamma) + B(k_\gamma) \sin^2\theta + C(k_\gamma) \sin^2\theta \cos\theta} \frac{d\sigma}{d\Omega} \Big|_{c.m.} \quad (3)$$

To obtain the uncertainty in the absolute cross section the combined uncertainty in the incident electron beam current, solid angle, and number of target nuclei per square centimeter (6.5%) should be combined in quadrature with the quoted uncertainties. Figure 2 shows that our (γ, p) cross section is in agreement with the ${}^3\text{H}(p, \gamma){}^4\text{He}$ measurements of Meyerhof, Suffert, and Feldman,⁷ which were normalized to the data of Perry and Bame.¹⁴ Figure 3 shows the ratios of $\sigma(\gamma, p)/\sigma(\gamma, n)$ from 30.0 to 51.8 MeV deduced from our experiment together with the BFK ratios.

In summary, our experiment has shown that in the energy interval of 30 to 51.8 MeV the ratio of ${}^4\text{He}(\gamma, p)$ to ${}^4\text{He}(\gamma, n)$ cross sections is 1.03 ± 0.04 . Our data strongly suggest, in the absence of a pronounced discontinuity in the ${}^4\text{He}(\gamma, n)$ cross section, that the ratio is not greatly different from 1 from threshold to 31 MeV.

The authors wish to thank Dr. E. G. Fuller for suggesting this experiment.

*National Research Council Postdoctoral Research Associate.

¹A. N. Gorbunov and V. M. Spiridonov, Zh. Eksp. Teor. Fiz. **34**, 866 (1958) [Sov. Phys. JETP **7**, 600 (1958)].

²E. G. Fuller, Phys. Rev. **96**, 1306 (1954).

³D. L. Livesey and I. G. Main, Nuovo Cimento **10**, 590 (1958).

⁴A. N. Gorbunov, Phys. Lett. **27B**, 436 (1968).

⁵I. G. Main, Nuovo Cimento **26**, 884 (1962).

⁶B. L. Berman, S. C. Fultz, and M. A. Kelly, Phys. Rev. C **4**, 723 (1971), and Phys. Rev. Lett. **25**, 938 (1970).

⁷W. E. Meyerhof, M. Suffert, and W. Feldman, Nucl. Phys. **A148**, 211 (1970).

⁸L. Busso, S. Costa, L. Ferrero, R. Garfagnini, L. Pasqualini, G. Piragino, S. Ronchi della Rocca, and A. Zani-

ni, Lett. Nuovo Cimento 3, 423 (1970).

⁹B. F. Gibson, private communication.

¹⁰E. M. Henley, in *Isospin in Nuclear Physics*, edited by D. H. Wilkinson (North-Holland, Amsterdam, 1969), p. 43.

¹¹D. M. Skopik and W. R. Dodge, to be published.

¹²B. F. Gibson and H. T. Williams, Nucl. Phys. A163, 193 (1971).

¹³W. R. Dodge and W. C. Barber, Phys. Rev. 127, 1746 (1962); B. Bosco and P. Quarati, Nuovo Cimento 33, 527 (1964); R. H. Dalitz and D. R. Yennie, Phys. Rev. 105, 1598 (1957).

¹⁴J. E. Perry and S. J. Bame, Jr., Phys. Rev. 99, 1368 (1955).

(O¹⁸, O¹⁶) Reaction on Mo Isotopes at Energies above the Coulomb Barrier*

C. Chasman, S. Cochavi,† M. J. LeVine, and A. Z. Schwarzschild

Brookhaven National Laboratory, Upton, New York 11973

(Received 7 January 1972)

The two-neutron transfer reaction (O¹⁸, O¹⁶) to the ground and first 2⁺ states of ^{94, 96, 98, 100}Mo has been measured at 55-, 60-, 70-, and 77-MeV projectile energy. Angular distributions and absolute cross sections are compared with the theory of Dar, which accounts for a large part of the variation of cross section with target mass number, energy, and the observed angular distributions. Evidence for multiple processes is exhibited in the excited-state cross sections.

One of the most useful tools for acquiring information concerning two-nucleon correlations in nuclei has been the two-neutron transfer reaction. Heavy-ion two-neutron transfer reactions offer a hope of providing such information with the additional constraint of taking place in the very peripheral regions of the nucleus. However, to extract useful spectroscopic information from the cross-section data, the details of the reaction mechanism must be determined. The elimination of large kinematic factors from the cross section, frequently not attempted, is necessary to avoid serious errors in interpretation. Nickles *et al.*¹ have reported on several heavy-ion transfer reactions on Zr targets at one energy. Although *above* the Coulomb barrier they showed that much of the *Q*-value dependence of their measured peak cross sections for neutron transfers is accounted for by the *sub-Coulomb* theory of Dar,² a qualitative discrepancy with this theory exists for their proton and two-proton transfer data. We report here on the two-neutron transfer reaction (O¹⁸, O¹⁶) on several even-*A* isotopes of Mo at energies above the barrier. In this effort to investigate some systematic behavior attributable to the reaction dynamics, we measured excitation functions and angular distributions for the ground and first 2⁺ states and compare them with the theory of Dar for energies above the barrier.

An O¹⁸ beam of 55, 60, 70, or 77 MeV was obtained using the Brookhaven tandem Van de Graaff

facility. Self-supporting targets of enriched Mo isotopes (~250 μg/cm²) were placed in a 30-in.-diam Ortec scattering chamber and viewed simultaneously at four angles with surface barrier detectors. The (O¹⁸, O¹⁶)-reaction *Q* value to the ground state varies from about 5.6 to 2.0 MeV in the range of targets of Mo⁹² to Mo⁹⁸. Identification of the emergent O¹⁶ particle was made on the basis of the positive *Q* value and the kinematic shift with angle, and no further particle identification was used. Spectra of the positive *Q* portion of the reactions Mo⁹⁴(O¹⁸, O¹⁶)Mo⁹⁶ and Mo⁹⁶(O¹⁸, O¹⁶)Mo⁹⁸ are shown in Fig. 1.

Data were reduced to absolute cross sections by normalization to the assumed pure Rutherford scattering at 40 MeV. Typical angular distributions at different energies are shown in Fig. 2. The shapes of the angular distributions for the reaction and elastic scattering are, within the typical experimental errors, independent of either the target or the state excited (ground state or first 2⁺ state), and are only functions of the bombarding energy. Thus, all the measured cross sections are adequately described by the curves of Fig. 2 and the values of the peak cross section as tabulated in Table I. Two very striking features are apparent: (i) At 60-MeV bombarding energy the peak cross section for the ground state rises by a factor of ~8 in going from Mo⁹² to Mo⁹⁸ targets, and (ii) the ratio of the 2⁺ to the ground-state cross section changes significantly with bombarding energy.